AIAA-2002-3720

# EXPERIMENTAL STUDY OF DEFLAGRATION-TO-DETONATION ENHANCEMENT TECHNIQUES IN A $H_2$/AIR PULSED-DETONATION ENGINE

T. R. Meyer,* J. L. Hoke,* and M. S. Brown†
Innovative Scientific Solutions, Inc.
Dayton, OH 45440-3638, USA

J. R. Gord‡ and F. R. Schauer*
Air Force Research Laboratory, Propulsion Directorate
Wright-Patterson Air Force Base, OH 45433-7103, USA

## Abstract

Experiments are performed on a number of deflagration-to-detonation (DDT) enhancement techniques for use in a $H_2$/Air pulsed-detonation engine (PDE). The mechanism, speed, and location of DDT for three configurations are considered, including a Shchelkin spiral, an extended cavity/spiral, and a co-annulus. High-speed digital imaging is used to track flame propagation, and simultaneous time-correlated pressure traces are used to record progress of the shock structure. It is found that DDT is initiated primarily through local explosions that are highly dependent on the particular geometry. In addition to various geometries, the effect of equivalence ratio and spark timing are also investigated.

## Introduction

The pulsed-detonation engine (PDE) has experienced renewed interest due to its simplicity, low cost, low weight, scalability, and potential for a broad range of operability.[1] To optimize PDE performance and enable high operating frequencies, it is important to reduce the percentage of fuel that is burned during low-pressure deflagration and, thus, to minimize the time required for deflagration-to-detonation transition (DDT). Direct initiation offers an alternative approach, but requires high input energies that reduce the overall system efficiency.

Deflagration-to-detonation transition has been the subject of scientific study for over a hundred years.[2] It is by nature extremely complex and highly three-dimensional, involving non-repeatable flame interactions with shocks, reflections, and boundary layers. For this reason, it is not easily studied with multi-point probes, spatially averaged measurement techniques, or single-frame imaging. To capture various features of shock-wave-flame interaction, an impressive series of DDT experiments have used high-frequency stroboscopic schlieren photography in smooth tubes filled with $H_2$ and air.[3,4] A common feature of the observed DDT events is the occurrence of an 'explosion-in-the-explosion' that spreads transversely into the shock compressed fuel-air mixture and leads to a self-sustained detonation.

Although much has been done to characterize detonation behavior in smooth tubes, DDT enhancement through the addition of obstacles is inherently very difficult to study because it involves turbulent combustion with complex boundary conditions.[5] Conventional detonability criteria using cell-size properties can determine if DDT is possible, but cannot determine if DDT is likely to take place.[6] The Shchelkin spiral, for example, while greatly reducing the time required for DDT in most cases, can also destroy the cellular structure[5] of the detonation or destabilize the coupling between the flame and the shock.[7]

While parametric studies on various obstacles can be performed,[7] a satisfactory description of why certain geometries are more effective than others is not yet available. For the purposes of developing DDT enhancement techniques for PDE applications, it is important to improve the understanding of how such

---

*Research Engineer, Member AIAA
†Physicist, Senior Member AIAA
‡Principal Research Chemist, Associate Fellow AIAA

# Report Documentation Page

*Form Approved*
*OMB No. 0704-0188*



| 1. REPORT DATE | 2. REPORT TYPE | 3. DATES COVERED |
|---|---|---|
| **2002** | | **00-00-2002 to 00-00-2002** |

| 4. TITLE AND SUBTITLE | 5a. CONTRACT NUMBER |
|---|---|
| **Experimental Study of Deflagration-to-Detonation Enhancement Techniques in a H2/Air Pulsed-Detonation Engine** | 5b. GRANT NUMBER |
| | 5c. PROGRAM ELEMENT NUMBER |
| 6. AUTHOR(S) | 5d. PROJECT NUMBER |
| | 5e. TASK NUMBER |
| | 5f. WORK UNIT NUMBER |
| 7. PERFORMING ORGANIZATION NAME(S) AND ADDRESS(ES) **Air Force Research Laboratory,Propulsion Directorate,Wright Patterson AFB,OH,45433** | 8. PERFORMING ORGANIZATION REPORT NUMBER |
| 9. SPONSORING/MONITORING AGENCY NAME(S) AND ADDRESS(ES) | 10. SPONSOR/MONITOR'S ACRONYM(S) |
| | 11. SPONSOR/MONITOR'S REPORT NUMBER(S) |

12. DISTRIBUTION/AVAILABILITY STATEMENT
**Approved for public release; distribution unlimited**

13. SUPPLEMENTARY NOTES
**The original document contains color images.**

14. ABSTRACT
**see report**

15. SUBJECT TERMS

| 16. SECURITY CLASSIFICATION OF: | | | 17. LIMITATION OF ABSTRACT | 18. NUMBER OF PAGES | 19a. NAME OF RESPONSIBLE PERSON |
|---|---|---|---|---|---|
| a. REPORT | b. ABSTRACT | c. THIS PAGE | | | |
| **unclassified** | **unclassified** | **unclassified** | | **11** | |

geometries interact with the flame and shock structures to produce conditions sufficient for DDT. The goal of the current investigation is to use short-exposure, high-speed digital imaging of flame luminosity and simultaneous pressure data to further this understanding for a number of DDT enhancement strategies. Emphasis is placed on visualizing the instantaneous flame front as a function of the geometry, operating conditions, and associated shock structure.

## Experimental Set-Up

The test facility, shown in Fig. 1, has been described previously by Schauer et al.[1] A modified General Motors Quad-4, dual-overhead-cam cylinder head is used for premixed fuel-air intake and spark ignition. The PDE is capable of operating with one to four tubes, and it can run at frequencies from single shot to tens of Hz. Only one of the four tubes shown in Fig. 1 is studied in the current investigation, and it is replaced with polycarbonate or quartz for optical access. Data collection is typically performed in single-shot mode for quartz tubes and up to five shots per run with polycarbonate tubes.

Detonation enhancement is achieved in the current investigation using three main approaches, as shown schematically in Fig. 2. The Shchelkin spiral consists of 3/16-inch mild-steel rod shaped into a 19-inch spiral and inserted into the entrance of a 2-inch inner diameter PDE tube. The extended cavity configuration extends the 3.5-inch bore of the cylinder head by about 8 inch in length before tapering to the 2-inch tube diameter. Based on preliminary measurements, this configuration has been modified to include a 54-inch Shchelkin spiral in the 2-inch section. For the co-annular geometry, 5- and 12-inch long tubes of 5/8-inch outer diameter are inserted at the entrance of the 2-inch PDE tube for a staged DDT approach.

High-speed digital imaging at rates up to 62,500 frames-per-second (fps) is employed using a Phantom v5.0 CMOS-based digital camera. At this framing rate, it has a field-of-view 32 pixels in height and 256 pixels in length and enables viewing of 8 tube diameters. The slowest framing rate used with the Phantom camera in the current investigation is 27,900 fps, for which the field of view of 32 × 1024 allows viewing of 32 tube diameters. Exposure times are kept at a constant value of 10 μs for all run conditions and framing rates.

Since the field-of-view of the Phantom camera is reduced at the higher framing rates, a second NMOS-based high-speed digital camera is also utilized in the current investigation and will be referred to as the Photron camera. It is capable of framing rates up to 40,500 fps with 64 × 64 pixels and 18,000 fps with 64 × 256 pixels. Typically, 18,000 fps is used in the current experiment and image magnification is adjusted so as to achieve about 32 pixels across the PDE tube and 256 pixels in length.

Through the use of these high-speed digital cameras, a time-history of the DDT process can be recorded during a single engine cycle. In addition, time-dependent pressure traces are collected simultaneously at several locations along the length of the PDE tube. The pressure traces provide a limited but unambiguous measure of the strength of the detonation wave during initiation and propagation. The camera is triggered from a pressure transducer located sufficiently downstream to ensure that the shock structure is well developed. This is necessary because the detonation and propagation events occur on the sub-millisecond time scale, and inherent variability in DDT timing prevents a priori phase-locking of the high-speed camera and PDE control system.

## Results

### Shchelkin Spiral

The detonation process resulting from a Shchelkin spiral is shown in false color in Fig. 3 for a $H_2$/air equivalence ratio of 1.0. The deflagration first becomes visible as a hot spot along a single spiral. Subsequent hot spots quickly become visible, and detonation is marked by a large increase in flame luminosity. These measurements show that DDT for this condition occurs within about 200 μs after the first explosion is detected. The effects of the retonation wave are also evident in Fig. 3. Hot spots induced by pressure-wave coalescence propagate *upstream* and cause the luminosity to increase significantly. Since the flame remains near the spirals during the DDT process, it is also likely that unburned pockets of fuel and air are also combusting as the retonation wave passes. Because the camera exposure was selected to highlight the transition process, camera saturation quickly occurs in the detonation and retonation regions and precludes further quantitative study in this sequence of images. It is possible to detect in other data sets, however, that the retonation wave is reflected back downstream and recompresses the combustion products.

It is also possible to track flame propagation along the spirals by focusing on the DDT region only and using the highest framing rate of 62,500 fps, as shown in Fig. 4. An important question regarding the geometry of the Shchelkin spiral is whether the flame propagates across the spirals as it would in a series of orifice plates, or whether it propagates along the spirals in a continuous fashion. This sequence of images shows quite clearly that the hot spots are propagating along the spirals, and helps to explain differences with the behavior of axisymmetric orifice plates (not presented

here). If a single geometric obstacle can provide an explosion that can enhance the flame-shock interaction, then a spiral obstacle provides a continuous line of explosions surrounding the deflagration as it propagates along the center of the tube.

The success of the Shchelkin spiral over concentric rings may be due to another an important feature of the transition process as visualized by Urtiew and Oppenheim.[4] They observed that the 'explosion-in-the-explosion' in smooth tubes produces a bow-shaped shock which reflects off the side walls and intensifies the flame-shock interaction. Unlike axisymmetric obstacles, the Shchelkin spiral can support additional helical modes that can propagate upstream as they grow and interact with the side walls. Compelling evidence for this mode of interaction is provided by frame-by-frame animations which show helical fluctuations in flame luminosity within the spiral during and after DDT. This increases the probability of coupling between the shock structure and turbulent flame propagation, thereby increasing the likelihood of DDT.

To verify proper coupling of the flame front and shock wave, simultaneous high-speed images and pressure traces are shown in Figs. 5 and 6 respectively. Once the flame advances ahead of the Shchelkin spiral, as shown in Fig. 5, it attains a nearly flat profile. This is partial indication that the flame is well-coupled to the shock front, as confirmed by the pressure traces in Fig. 6 showing that the flame and shock fronts arrive nearly simultaneously at the pressure transducer locations. Note that the pressure traces follow the expected temporal profile, with a very high initial von Neumann spike and a subsequent Chapman-Jouguet (C-J) peak after the initial shock. The speed of the shock is such that it is possible to miss the peak of the pressure rise, as shown in the curve for PT4 in Fig. 6.

Extended Cavity / Shchelkin Spiral

Initial tests found that the extended cavity geometry did not significantly enhance DDT. Endview images were collected at several conditions for this configuration, and show that local hot spots are generated but produce weak detonations with speeds up to 800 m/s.

For the data presented here, a 54-inch spiral was added just after the extended cavity for the following reasons: (1) to determine if the increased initial heat release and hot spots generated by the extended cavity can reduce the time required for DDT and (2) to determine the effect of a lengthened spiral.

As shown in Fig. 7 for unity equivalence ratio, DDT is achieved shortly after the exit of the cavity (just to the left of each image). Since the flame is accelerated due to the geometry of the cavity, interaction with the spiral leads to an immediate transition. This case differs significantly from that of a pure Shchelkin spiral geometry. This is shown by the decaying detonation front, which begins as the flame front loses its flat character at PT3. This decay can be attributed to two main possibilities: (1) once DDT has taken place, the spiral interferes with the flame-shock coupling, or (2) the long spiral results in residual air remaining in the tube and causing lower than expected equivalence ratios.

Evidence for the former is provided in the pressure traces of Fig. 8. The pressure pulse for PT4 arrives several microseconds before the visible flame front, indicating that the primary flame-shock interaction has been disrupted. The flame-speed and luminosity quickly decay in the aftermath of this disruption, although local explosions are occurring which continue to drive the flame forward as a weak detonation. These local explosions are evident in the high-speed images of Fig. 7 as well as in the pressure spikes for PT5 in Fig. 8.

The flame speeds from the Shchelkin spiral geometry of Fig. 5 and the cavity/spiral geometry of Fig. 7 are shown for comparison in Figs. 9(a) and (b), respectively. For the Shchelkin spiral configuration of Fig. 9(a), the C-J velocity of about 2000 m/s is achieved after about seven tube diameters downstream of the engine block. This velocity is verified by measurements of the shock-wave speeds between pressure pulses, which are on the order of 2000 m/s as far as PT6 near the exit of the tube.

For the cavity/spiral configuration of Fig. 9(b), the flame enters the viewing area at nine tube diameters as a C-J detonation, but the flame speed varies tremendously. Velocities greater than the C-J velocity do not necessarily represent overdriven detonations, but could also represent the more intermittent nature of flame propagation via shock-induced local explosions. This intermittency indicates that the flame and shock are not well coupled, although strong local explosions drive the flame periodically to C-J velocities up to about 22 tube diameters downstream. Pressure traces indicate that the shock-wave is already below C-J conditions between PT3 and PT4, with a measured transit time corresponding to 1800 m/s. It drops further to about 900 m/s between PT4 and PT5.

Co-Annulus

The co-annulus shown previously in Fig. 2 was implemented due to promising results from numerical simulations. The idea is to initiate a detonation in the smaller tube first, which can then drive a detonation in the larger tube.

The results of a 5-inch long inner tube and a 12-inch long inner tube are shown in Figs. 10(a) and (b). The experimental data did not show a strong enhancement

of the DDT process. For the 5-inch tube, a hot spot develops *outside* the tube near its downstream tip. The flame from the central tube finally exits as a strong flame front, but it enters a burned-gas medium. For the 12-inch tube of Fig. 10(b), a hot spot occurs at the downstream tip of the inner tube, but in this case is also joined by the flame exiting the inner tube. Combustion pressures of nearly one-third that expected for a C-J detonation indicate that the flame is accelerated but does not achieve DDT. The measured flame velocity reaches about 520 m/s, which is well below the velocity of about 2000 m/s expected for stoichiometric mixtures of $H_2$/air.

Subsequent analysis of the numerical results indicates that the flame from the inner tube can be strongly dissipated unless its diameter is greater than one-half the diameter of the main tube. Subsequent experiments to verify this prediction are the subject of ongoing study.

Effects of Equivalence Ratio and Spark Timing

In addition to the effects of geometry on DDT, it is also of interest to study the effect of various operating conditions. For the Shchelkin spiral geometry, varying the equivalence ratio between 0.9 and 1.3 had an impact on the location of DDT, as expected, but did not affect the nature of the transition. The shortest distance required for DDT occurs at stoichiometric conditions and extends further downstream as the equivalence ratio becomes progressively lean or rich. For an equivalence ratio of 1.3, for example, DDT takes place three tube diameters further downstream near the end of the 19-inch Shchelkin spiral.

For the extended cavity/spiral configuration, varying the equivalence ratio between 0.75 and 1.0 had a similar effect. For stoichiometric conditions, the transition occurs almost immediately in the field-of-view, as shown in Fig. 7. At an equivalence ratio of 0.75, the transition occurs about two tube diameters further downstream. Despite these differences in location of DDT, the detonation speeds remain within about 2% of the theoretical C-J velocities once the self-sustained condition is achieved.

The primary effect of spark timing is to change the $H_2$/air mixture further downstream in the PDE tube. Large differences in the location of DDT are not detected in the current experiments, and it is found that the C-J velocities for early and late spark timings agree to within about 5%. The detonation wave for late spark timing, however, has difficulty propagating to the end the tube. This is attributed primarily to mixing with ambient air near the end of the tube caused by pulsing of the fresh $H_2$/air mixture. Thus, wave speeds near the end of the PDE tube drop to the level of weak detonations as the spark timing is progressively increased. These data highlight the importance of measuring fuel mixture fraction near the end of the PDE tube as a function of time during PDE operation.

## Conclusions

An experimental study of three DDT enhancement techniques and different operating conditions has been performed using simultaneous high-speed digital imaging and pressure-transducer data. It is found that local explosions in the Shchelkin spiral geometry propagate along the spirals and behave in a fundamentally different manner when compared with local explosions produced by axisymmetric obstacles. In addition, it is shown that the continuous spiral geometry leads to transverse and helical modes that may enhance coupling between the flame and shock fronts. It is found that adding an extended cavity before the Shchelkin spiral leads to strong early detonations that then decay more quickly as compared with a simple Shchelkin spiral geometry. The co-annular geometry with inner tube diameters of less than half the main tube diameter did not lead to strong detonations and is under further investigation. Finally, equivalence ratio was found to change the location but not the nature of the transition, and spark timing was found to impact the progression of the detonation wave near the exit of the PDE tube. These studies provide a phenomenological description of the effects of geometry and various operating parameters on the flame-shock interaction during and after the DDT process.

## Acknowledgments

The authors would like to acknowledge R. P. Bradley and C. Rice of ISSI and co-op students Matt Slagel, Jason Parker, and Brian Frankey for their assistance in the set-up and operation of the PDE facility. We also thank V. R. Katta of ISSI for his modeling efforts and for useful discussions regarding the deflagration-to-detonation transition process. This work is supported in part by U. S. Air Force Contract F33615-00-C-2068.

## References

[1] F. Schauer, J. Stutrud, and R. Bradley, "Detonation Initiation Studies and Performance Results for Pulse Detonation Engine Applications," AIAA Paper No. 2001-1129, *39th AIAA Aerospace Sciences Meeting and Exhibit*, Reno, Nevada, Jan. 8-11, 2001.

[2] E. Mallard and H. Le Chatelier (1883), "Recherches Experimentales et Theoriques sur la Combustion des Melanges Gaseoux Explosifs," *Ann. Mines* 8(4): 274-568.

[3] A. K. Oppenheim, P. A. Urtiew, and F. J. Weinberg, (1966) "On the Use of Laser Light Sources in Schlieren-Interferometer Systems," *Proc. Roy. Soc. London*, A291:279.

[4] P. A. Urtiew and A. K. Oppenheim (1966), "Experimental Observations of the Transition to Detonation in an Explosive Gas," *Proc. Roy. Soc. London*, A291:13.

[5] J. H. S. Lee, "On the Transition from Deflagration to Detonation," Dynamics of Explosions, Vol. 106: Progress in Astronautics and Aeronautics, Martin Summerfield, Editor, American Institute of Aeronautics and Astronautics, Inc., New York, 1986.

[6] O. Peraldi, R. Knystautas, and J. H. Lee, "Criteria for Transition to Detonation in Tubes," 21st Symposium (International) on Combustion, The Combustion Institute, pp. 1629-1637.

[7] R. P. Lindstedt and H. J. Michels (1989), "Deflagration to Detonation Transitions and Strong Deflagrations in Alkane and Alkene Air Mixtures," *Combustion and Flame* 76:169-181.

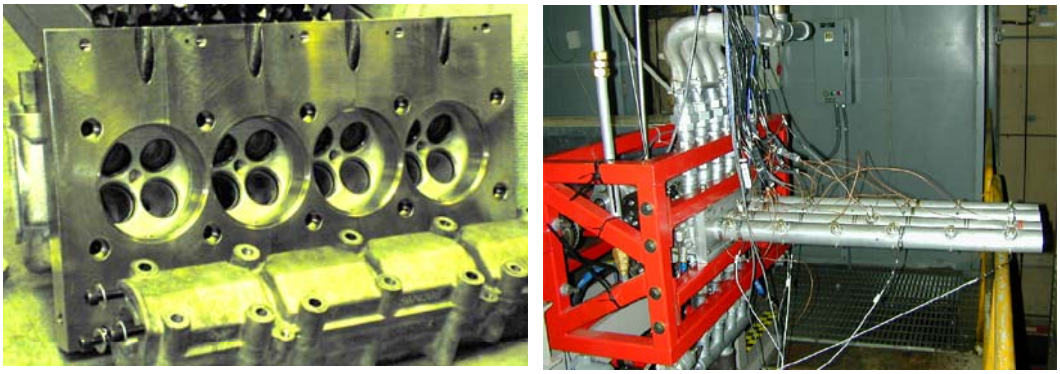

**Fig. 1. Quad-4-based PDE during assembly (left) and as installed. Only one of the tubes is studied for the current investigation and is replaced with polycarbonate or quartz for optical access.**

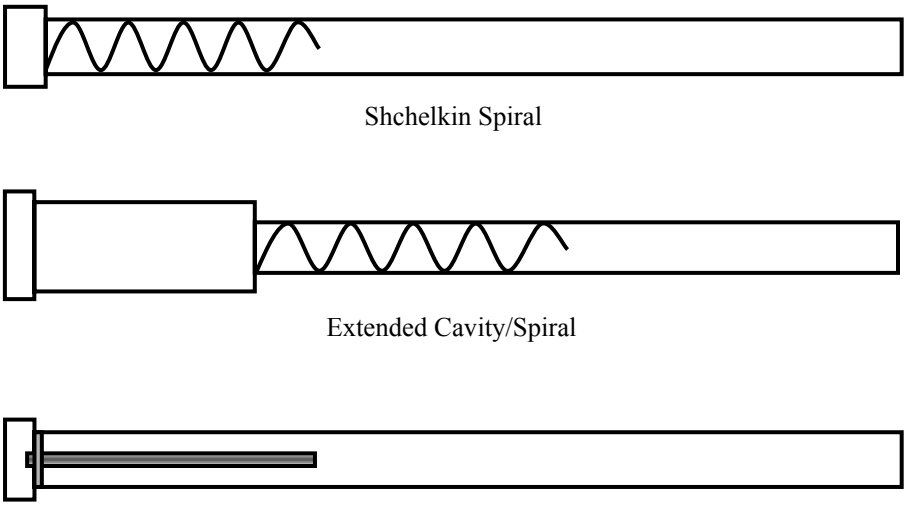


**Fig. 2. Schematic of DDT enhancement techniques discussed in the current study. Sketches are not to scale.**

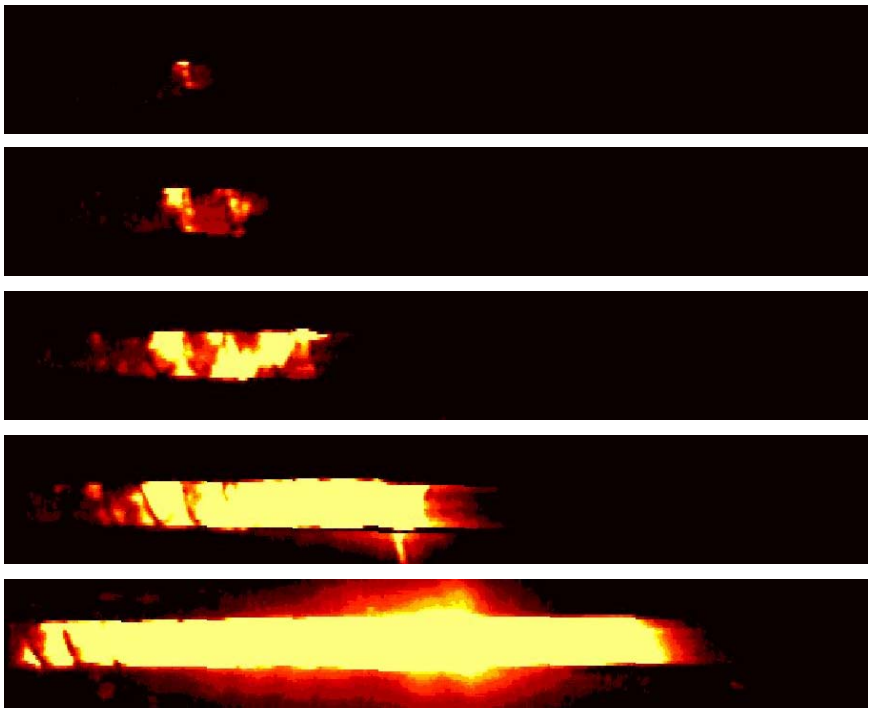

**Fig. 3. High-speed images of DDT at 18,000 fps for a Shchelkin spiral at $\phi$=1. Images are spaced 55.5 μs apart.**

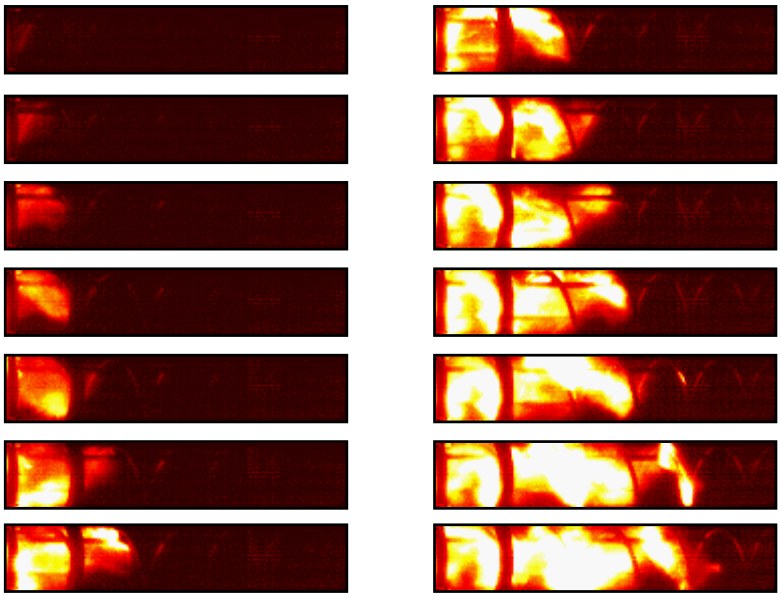

**Fig. 4. Sequence of high-speed digital images at the highest framing rate of 62,500 fps for a Shchelkin spiral geometry. The flame front is clearly shown to take place along the spirals.**

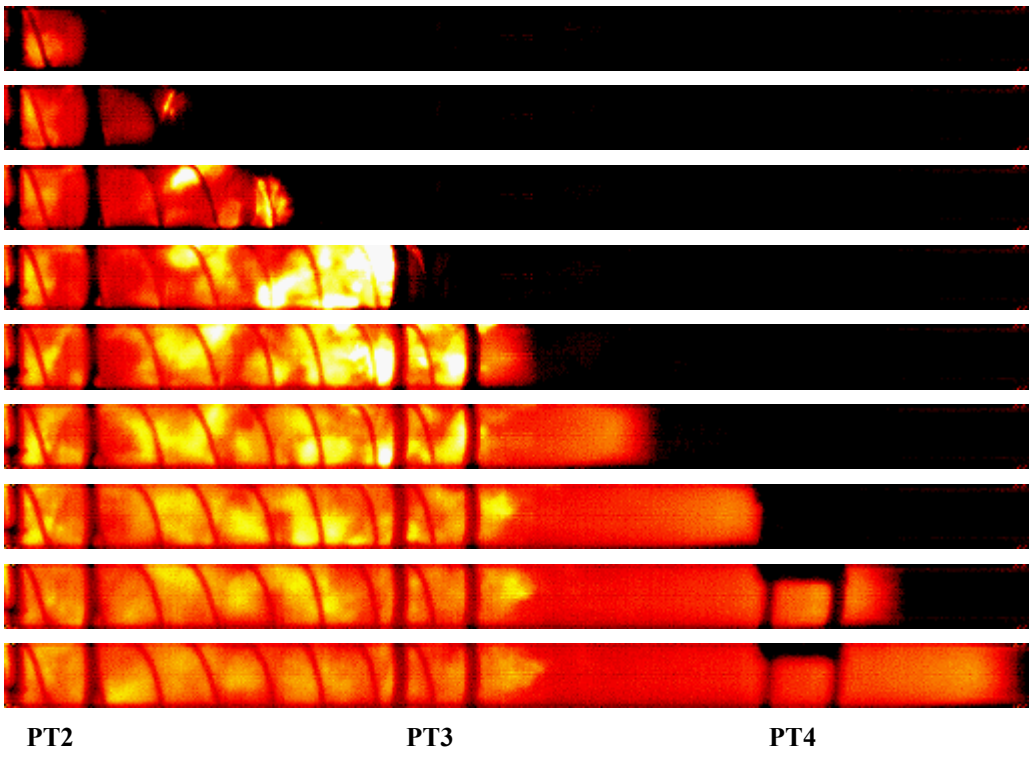


**Fig. 5. Image sequence showing DDT initiated by a Shchelkin spiral with pitch of 1 tube diameter and length of 9.5 tube diameters. Images are spaced 50 μs apart in time and begin 5 μs after PT2 is triggered. Equivalence ratio is 1.0. Pressure transducer locations are labeled as PT2 to PT4.**

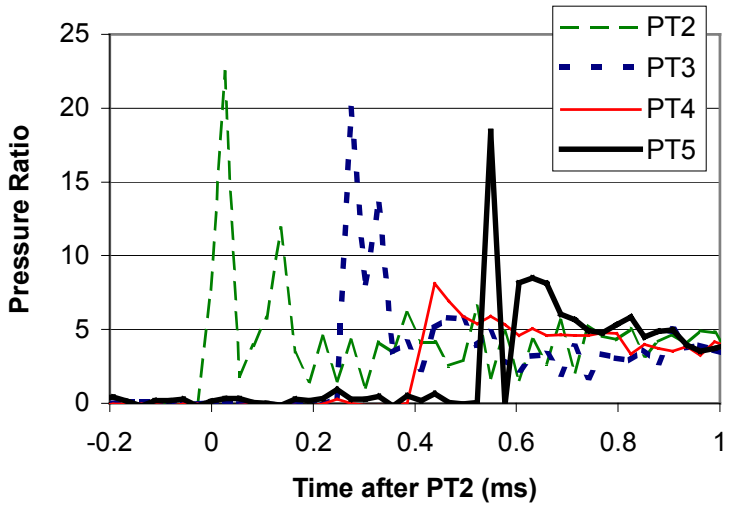


**Fig. 6. Pressure traces for the Shchelkin spiral geometry of Fig. 5.**

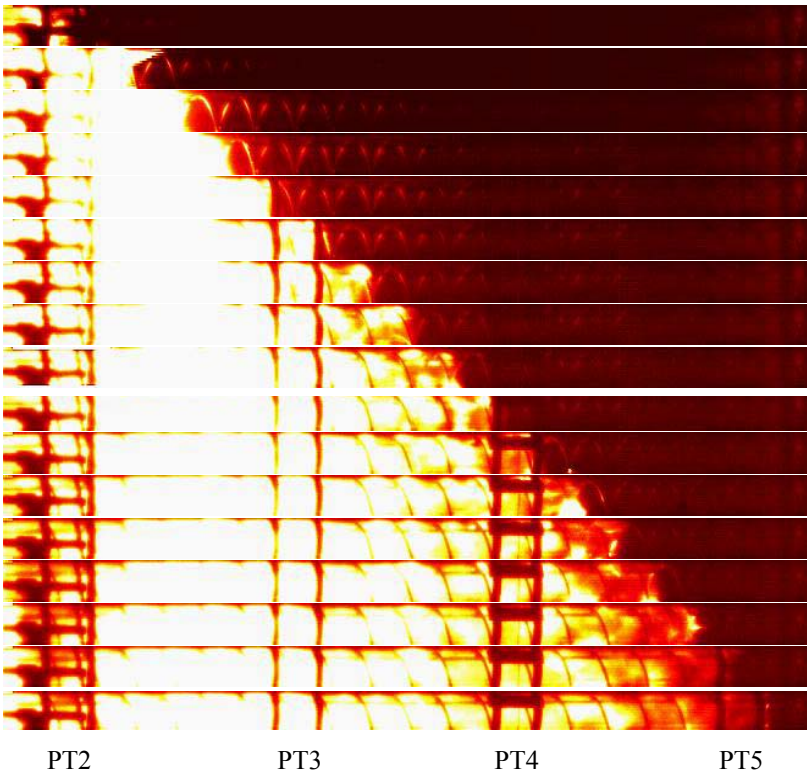


**Fig. 7. Sequence of high-speed digital images for an extended cavity/spiral geometry.**

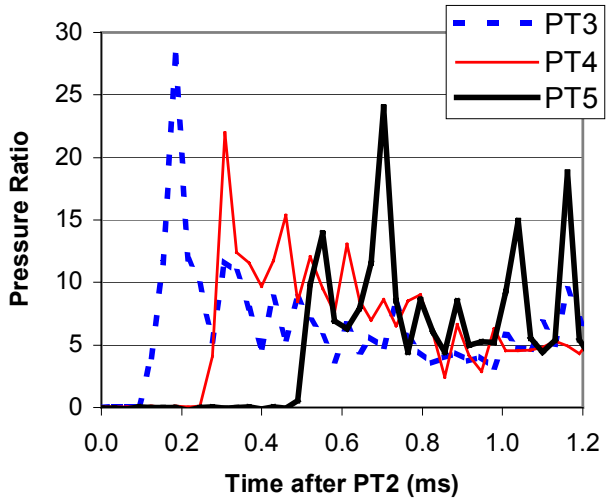


**Fig. 8. Pressure traces for the extended cavity/spiral geometry of Fig. 7.**

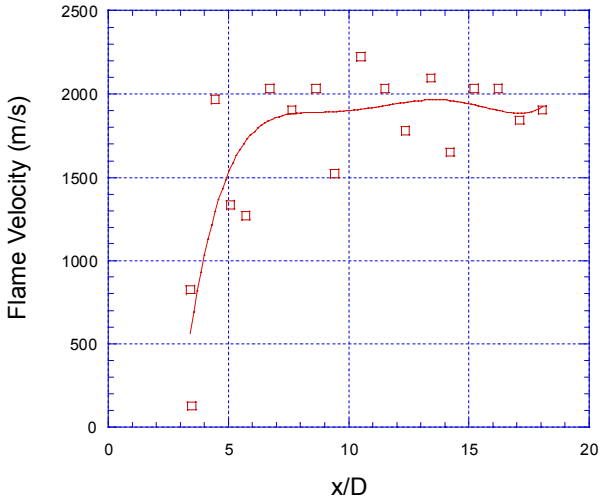


**(a)**

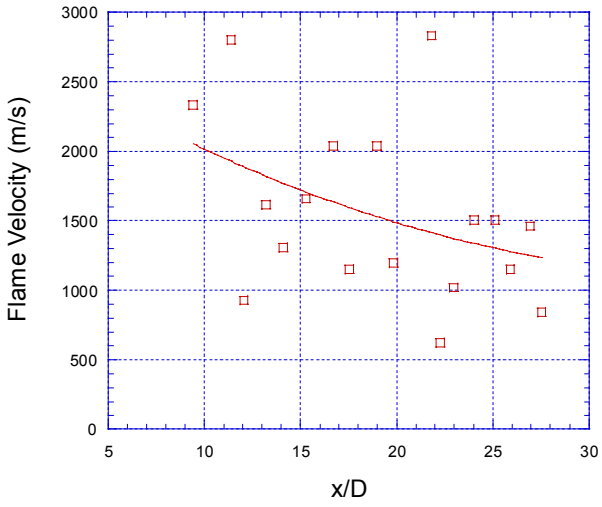


**(b)**

**Fig. 9. Flame speeds for the (a) Shchelkin spiral geometry of Fig. 5 and (b) the extended cavity/spiral geometry of Fig. 7.**

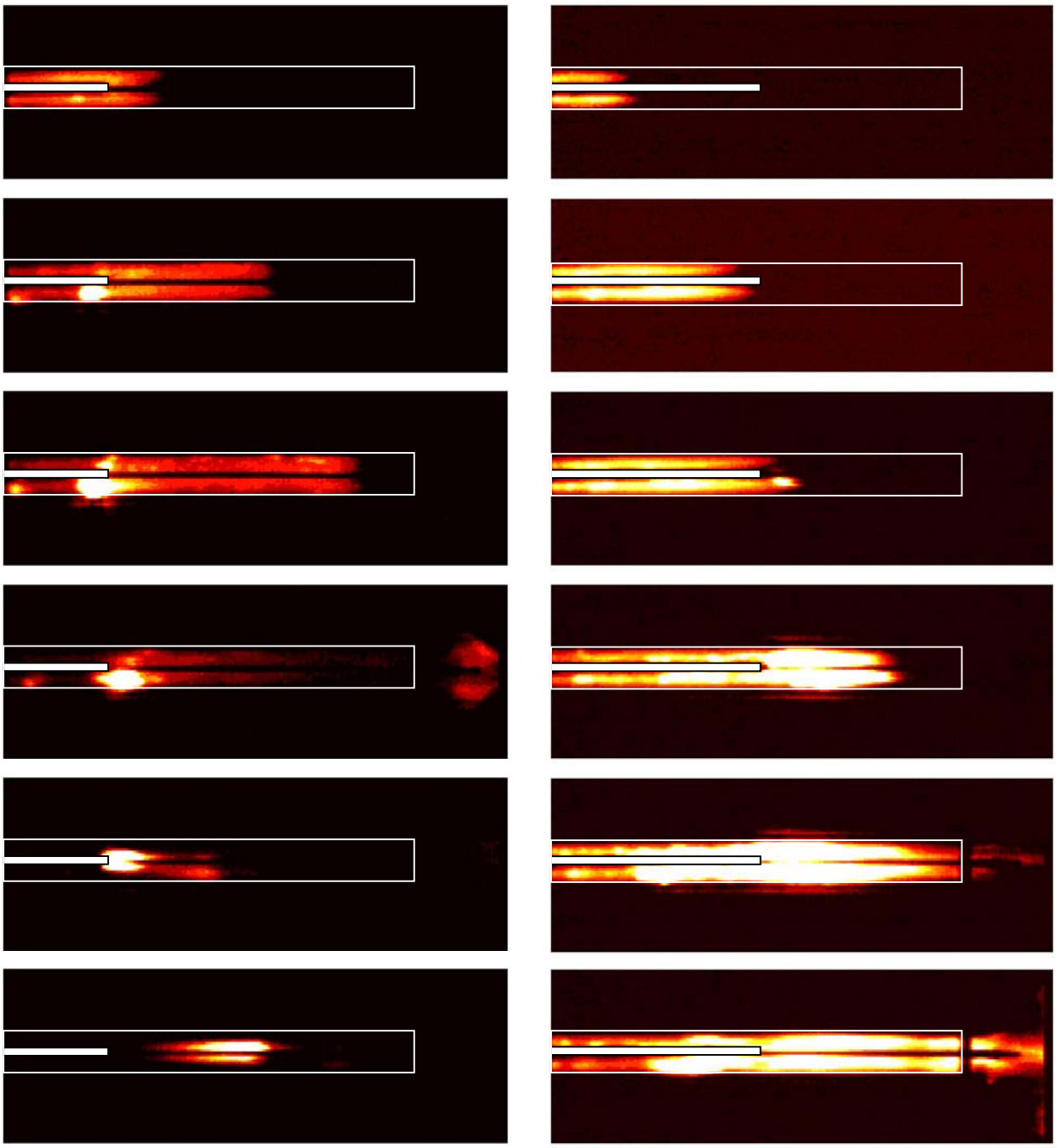

(a) (b)

**Fig. 10. Image sequence showing co-annular tube DDT enhancement geometry with tube length of (a) 2.5 tube diameters and (b) 6 tube diameters. Equivalence ratio is 1.0. Maximum velocity of 520 m/s achieved for (b). Outlines of main and inner PDE tubes shown in white.**